Cement and Concrete Research 42 (2012) 736–744

Contents lists available at SciVerse ScienceDirect

Cement and Concrete Research

journal homepage: http://ees.elsevier.com/CEMCON/default.asp

Study of the retarding mechanism of linear sodium polyphosphates on α-calcium sulfate hemihydrate

V. Nilles, J. Plank *

Chair for Construction Chemicals, Technische Universität München, 85747 Garching, Germany

ARTICLE INFO

Article history:
Received 21 July 2011
Accepted 16 February 2012

Keywords:
Retardation (A)
Hydration (A)
Pore solution (B)
Calcium sulfate hemihydrate

ABSTRACT

Linear sodium polyphosphates possessing different average chain lengths were characterized and studied as retarder for α-calcium sulfate hemihydrate. Their effect on the hydration kinetics of aqueous α-$CaSO_4 \cdot 0.5H_2O$ pastes was quantified by heat flow calorimetry, mini slump test and determination of time-dependent degree of hydration. Already at very low dosages (0.025% bwob) polyphosphates strongly retard hydration of hemihydrate. The retarding effect decreases with increasing chain length. Interaction between polyphosphates and calcium ions and Ca^{2+} concentration dependent formation of insoluble precipitates were studied via pH and turbidity measurements. Additionally, the influence of polyphosphates on individual hydration steps (binder dissolution and gypsum precipitation) was determined. It was found that the working mechanism of polyphosphates mainly relies on a strong decrease of binder dissolution rate while delayed gypsum precipitation from the solution and inhibition of dihydrate crystal growth by adsorption of polyphosphate play a minor role.

1. Introduction

Sodium polyphosphates present a versatile group of functional additives which are used in numerous industrial applications [1]. Their main functional properties include buffering, calcium binding, dispersing, water retaining and the so-called "threshold capability". Generally, they are fabricated via condensation of orthophosphates at elevated temperature. In this process, orthophosphates are annealed at 625 °C which is above their melting point. As an example, Fig. 1 presents the principle reaction steps occurring during the condensation of NaH_2PO_4 to yield a linear polyphosphate exhibiting a certain chain length distribution. At increased temperature, two orthophosphate molecules first react to form a diphosphate, releasing one water molecule. Through repeated condensation steps, a linear chain is built until the reaction in the melt is quenched by rapid cooling to room temperature. The polyphosphates obtained from this process are amorphous, glassy materials.

The properties of polyphosphates (especially the average chain length) can be adjusted through several parameters including reaction temperature, condensation time, the cooling rate applied to the melt and, most important, the monomer composition [2,3]. For example, addition of Na_2HPO_4 instead of NaH_2PO_4, results in shorter chains as it functions as chain terminating agent. The reason is that in Na_2HPO_4, only one ≡P–OH group is present which can undergo condensation. Once reacted, no further condensation is possible.

Applications of sodium polyphosphates primarily derive from their specific properties in aqueous solution. A major use is as scale inhibitor and water softening agent [4]. In detergent formulations, polyphosphates greatly increase the efficacy of surfactants because of their calcium binding capability. Apart from their contribution to water eutrophication, polyphosphates generally are non-toxic to humans and the environment [5]. They are even used in the food industry and identified there as E 452. Moreover, in the paint and varnish industry polyphosphates are applied to disperse and stabilize pigment suspensions [1]. Their strong dispersing effect is also employed in many other applications to adjust the rheological properties of e.g. aqueous calcium carbonate [6], mixed mineral [7] and especially clay suspensions (e.g. in drilling fluids used by the oil industry) [8–11].

In building materials, polyphosphates can be used as retarders for calcium sulfate-based binders. They provide a versatile alternative to common retarding admixtures which are based on α-hydroxy carboxylic acids such as tartaric or citric acid [12,13]. Their working mechanism has been studied extensively and was found to rely on calcium complexation and molecular interaction between the acids and calcium sulfate dihydrate nuclei formed in the initial stages of the hydration process. There, growth of the $CaSO_4 \cdot 2H_2O$ nuclei is inhibited by sorption of retarder molecules on the crystal faces. This way, the final setting is delayed [14–17]. Also, polymers possessing specific functionalities such as hydroxy, amino or phosphonate groups are known to be effective retarders. Such examples are protein

* Corresponding author at: TU München, Lehrstuhl für Bauchemie, Lichtenbergstr. 4, 85747 Garching, Germany. Tel.: +49 89 289 13150.
E-mail address: sekretariat@bauchemie.ch.tum.de (J. Plank).

0008-8846/$ – see front matter © 2012 Elsevier Ltd. All rights reserved.
doi:10.1016/j.cemconres.2012.02.008

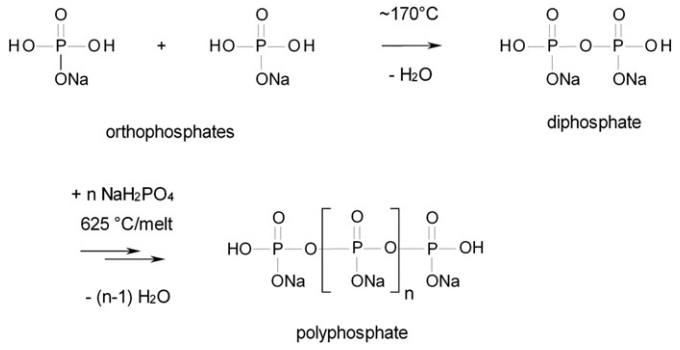

Fig. 1. Condensation of NaH_2PO_4 into a linear polyphosphate.

hydrolysates and synthetic polycondensates prepared from pyrrolidone and formaldehyde [18,19].

So far, no study describing the effectiveness and working mechanism of linear polyphosphates with regard to hydration inhibition of calcium sulfate hemihydrate binder has been published.

Here, three linear sodium polyphosphates possessing different chain lengths were compared with respect to their retarding effectiveness on α-$CaSO_4 \cdot 0.5H_2O$. Retardation was probed via measurement of paste flow (workability or open time), degree of hydration as well as strength development. To understand their working mechanism, their interaction with calcium ions in solution was probed and a correlation between their chemical structure (chain length), their retarding effectiveness and calcium precipitation ability was established. Furthermore, the chain length dependent influence of the polyphosphates on individual hydration steps, namely on binder dissolution and on gypsum precipitation, was studied through conductometry. From the results, a model for the retarding mechanism of polyphosphates in dependence of the chain length is proposed.

2. Materials and methods

2.1. Materials

2.1.1. Polyphosphates

Three commercial sodium hydrogen polyphosphate samples (Budit 7, 8 and 9) supplied by "Chemische Fabrik Budenheim KG" (Budenheim, Germany) were tested. The products are white, hygroscopic and water-soluble powders.

In all experiments, freshly prepared aqueous solutions of the polyphosphates were used to exclude any influence from different dissolution rates or unwanted hydrolysis and carbonation during prolonged storage.

2.1.2. α-Calcium sulfate hemihydrate

α-$CaSO_4 \cdot 0.5H_2O$ (purity ~97%) prepared from FGD gypsum was supplied by Knauf Gips KG (Iphofen, Germany). The average particle size (d_{50} value) was found at 36 μm, and the density was 2.8 g/cm^3. Its specific surface area (BET, N_2) was determined to be 24,000 cm^2/g.

2.2. Methods

2.2.1. ^{31}P NMR spectroscopy

Liquid state ^{31}P NMR spectroscopy was performed in D_2O as a solvent on a Bruker DPX — 400 MHz instrument (Bruker BioSpin MRI GmbH, Ettlingen, Germany) operated at 161.992 MHz. As internal standard, aqueous phosphoric acid (85%) was added in a sealed capillary to the tube holding the polyphosphate sample to be tested.

2.2.2. Heat flow calorimetry

Binder hydration was tracked in presence and absence of polyphosphates using a *TAM Air* isothermal heat conduction calorimeter (Tam Air, Thermometric, Järfälla, Sweden). In a typical experiment, 4 g of hemihydrate was weighed into a 10-mL plastic container and 1.32 mL of DI water or polyphosphate solution was added (w/b ratio = 0.33). The container was sealed and the content was intensively mixed for 1 min using a vortex tumbler. The homogenized sample was placed in the calorimeter at 20 °C and time-dependent heat flow was recorded. The data were collected and evaluated using the *TAM Air assistant* software. Heat flow values were calculated in mW/g by dividing the raw data by a factor of 4.

2.2.3. Mini slump test

Fluidity of the calcium sulfate hemihydrate pastes was measured using the mini slump test according to DIN EN 1015. A water-to-binder ratio (w/b) of 0.33 yielding a spread flow of 18 ± 0.5 cm was established as reference. The test procedure was as follows: 300 g of hemihydrate was added to the mixing water which in some experiments contained the dissolved polyphosphates. This was followed by manual stirring with a spoon for 2 min. Next, the paste was transferred into a VICAT cone (height 40 mm, top diameter 70 mm, bottom diameter 80 mm) placed on a glass plate and was then vertically lifted. The resulting spread of the paste was measured twice; the second measurement being perpendicular to the first. The final spread flow value was taken as the average of the two values measured. For time dependent paste flow behavior, after each measurement the paste was quantitatively collected in a porcelain cup and covered with a moist towel. Flow values were taken every 5 min, and the paste was stirred for 2 min prior to testing.

2.2.4. Degree of hydration of α-$CaSO_4 \cdot 0.5H_2O$

To assess the retarding capacity of the individual polyphosphates, time dependent degree of hydration (DoH) was determined gravimetrically by quantifying the amount of calcium sulfate dihydrate (DH) formed. Following the procedure employed in the mini slump test, $CaSO_4 \cdot 0.5H_2O$ pastes were prepared. After defined time intervals, small portions (5–10 g) thereof were added to an excess of isopropanol (~500 mL) and stirred with a spoon for 30 s. By using this method, hydration of the binder was stopped. Samples which already had solidified were transferred into a mortar, wetted with 2.5 mL isopropanol, crushed with a pestle and then diluted with 500 mL of isopropanol. The suspensions were then filtered under vacuum and the residues were taken up twice again with 25 mL of isopropanol each. The solids were first dried for 1 h at room temperature, followed by drying over night in a drying oven at 60 °C. Thereafter, all samples were kept in an exsiccator (in vacuo) prior to analysis.

For DoH measurement, a defined part (~1–2 g) was weighed into a crucible and calcined in an oven (Carbolite CSF 12/13, London, England) for 12 h at 700 °C. During this period, calcium sulfate hemihydrate and dihydrate (which were assumed to be the sole phases present) release their crystal water yielding anhydrite (Eq. 1). After cooling to ambient, the samples were weighed and the loss on ignition (LOI) was calculated.

$$x\,CaSO_4 \cdot 0.5H_2O + y\;CaSO_4 \cdot 2H_2O \rightarrow (x+y)\,CaSO_4 + (0.5x+2y)\,H_2O\uparrow. \quad (1)$$

The degree of hydration (DoH) was defined as percentage of calcium sulfate dihydrate formed during binder hydration relative to the amount of anhydrite resulting from the drying of the hydration product which contained a mixture of hemihydrate and dihydrate (Eq. 2).

$$DoH[\%] = \frac{n(DH)}{n(CaSO_4)} \cdot 100 = \frac{y}{(x+y)} \cdot 100. \quad (2)$$

It was assumed that the loss on ingnition (LOI) was exclusively owed to the release of water from the hydrates ($n(H_2O) = (0.5x+2y)\,(H_2O) = (m_i - m_f)/M\;(H_2O)$, where n is the molar amount of the respective

fraction, m_i is the initial weight of the sample and m_f is the final weight of the sample). Moreover, using XRD measurement it was confirmed that the residue remaining after thermal treatment was pure anhydrite ($n(CaSO_4) = (x+y)\ (CaSO_4) = m_f/M\ (CaSO_4)$; where M ($CaSO_4$) is 136 g/mol and M ($H_2O$) is 18 g/mol). Employing this method, the molar ratio between evaporated water and formed anhydrite, $n(H_2O)/n(CaSO_4)$ which can also be expressed by the quotient $(0.5x+2y)/(x+y)$, can be determined. Using this method, the percentage of DH formed as a result of hemihydrate hydration can be calculated according to Eq. (3):

$$DoH\ [\%] = \frac{\left(\frac{n(H_2O)}{n(CaSO_4)}\right) - 0.5}{1.5} \cdot 100 \quad (3)$$

To determine the accuracy of this method, random samples were additionally subjected to thermogravimetric analysis using a NETZSCH STA 409 Netzsch instrument (Selb, Germany). Comparison of the results obtained from both methods produced a difference of ±4% for the DoH values which were deemed to be acceptable.

2.2.5. Compressive and tensile strength

To evaluate the influence of the polyphosphates on the mechanical properties of the hardened samples, compressive and bending tensile strengths were determined. Rectangular specimens (40 mm × 40 mm × 160 mm) were prepared according to DIN 1168-2. Within 1 min, 2 kg of hemihydrate powder was added to 660 mL of DI water or the respective polyphosphate solution placed in the steal cup. The suspension was mixed manually with a spoon for 1 min and then placed in a *Hobart N-50* mixing device (Hobart, Offenburg/Germany) for 2 min of homogenization at low intensity. Subsequently, the pastes were filled into molds and entrained air was removed by lifting the mold at the front end by ~1 cm and subsequent dropped. This procedure was repeated 5 times. Excess paste was removed by scratching the surface with a trowel. The samples were covered with a plastic foil and stored at 23 ± 0.5 °C and 65% relative humidity. After 24 h, the molds were dismantled and the specimens were stored at the same climate conditions. Compressive and bending tensile strengths were measured after 3, 7 and 28 days following DIN EN 1015-11. For tensile strength, 3 independent samples were tested and the average value was calculated. While for the compressive strength values, the average of six independent samples were taken.

2.2.6. Conductometry

Hydration of α-HH was also tracked by conductometry. 10 g of α-hemihydrate was added under stirring to 200 mL of DI water or polyphosphate solution using a water-to-solids ratio of 20 to 1. Time-dependent evolvement of the conductivity of the suspensions was measured employing a *Qcond 2200* instrument (VWR international/Darmstadt, Germany). All experiments were conducted at room temperature (22.5 ± 2.5 °C) at a stirring speed of 400 rpm of the magnetic stirrer.

2.2.7. Quantification of phosphate concentration in solution

The concentration of polyphosphate in solution was determined by hydrolyzing the polyphosphate to orthophosphate and subsequent measurement of the orthophosphate concentration by using the molybdenum blue method [20,21]. This test was conducted according to DIN EN ISO 6878 (D11).

First, a calibration curve for each individual polyphosphate sample was developed. For this purpose, 0.1 g of the polyphosphates was dissolved in 10 mL of DI water. After addition of 3 mL of concentrated sulfuric acid, the solution was heated for 5 min to the boiling point. At this pH (<2) and temperature, polyphosphate hydrolyses quantitatively to the respective orthophosphate which can then be analysed by the molybdenum blue method. After cooling to ambient, pH of the solution was adjusted to pH 2–3 using aqueous 30 wt.% sodium hydroxide. Then, the sample was filled up to 100 mL in a volumetric flask using DI water. From the resulting solution 1 mL was transferred to a 100 mL volumetric flask and filled up to the marker with DI water. This solution was used as stock solution for serial dilution to obtain the calibration curve for the individual polyphosphates. From the stock solution, dilutions were made using DI water to obtain solutions containing orthophosphate amounts corresponding to concentrations of 0.15625–10 mg/L of the polyphosphate. From the extinctions of the reference solutions measured at 880 nm, a calibration curve was developed.

Phosphate concentrations present in the pore solution of the binder pastes were determined starting from pastes prepared according to the mini slump test (w/b = 0.33). At specific time intervals, pore solution was collected through vacuum filtration of the paste using a filter paper. The solution was taken up with a syringe and filtrated a second time by pressing through a syringe filter (pore size < 0.2 μm) to remove microcrystalline calcium phosphate precipitates. A definite volume (2–10 mL) of the pore solution obtained containing an unknown phosphate concentration was boiled with sulfuric acid, and diluted with water as described above.

Separately, an aqueous solution was prepared from 6.5 g ammonium heptamolybdate and 0.175 g potassium antimony oxide tartrate in 200 mL of DI water. Next, 50 mL of concentrated sulfuric acid was added. Furthermore, an aqueous solution of 10 wt.% ascorbic acid was prepared and kept in the refrigerator in a brown glass. Then, 1.3 mL of the stock solution for calibration or of the pore solution containing the unknown phosphate concentration, 100 μL of the molybdate solution and 100 μL of the ascorbic acid solution were combined in a cuvette and mixed with a pipette. After 20 min, the solution had fully developed its blue color and absorption was measured at a wavelength of 880 nm (Varian Cary WinUV–Spectrometer, Varian Inc., Palo Alto, California).

The amount of orthophosphate present in the pore solution was determined through comparison of the extinction measured for the sample with the ones from the calibration curve. The amount of phosphate was calculated from the difference between initial concentration and concentration found in the pore solution after contact with the binder.

2.2.8. Precipitation of calcium polyphosphates

This experiment was conducted to study the interaction of the polyphosphates with calcium ions. 0.1 g of the polyphosphate sample was dissolved in 100 mL of DI water. Separately, 3.675 g of $CaCl_2 \cdot 2H_2O$ was dissolved in ~95 mL of DI water. The pH of this solution was adjusted to 8.5 using $NaOH_{(aq)}$. The solution was transferred into a volumetric flask and filled up to 100 mL with DI water. The $CaCl_2$ solution obtained exhibits a Ca^{2+} ion concentration of 10 g/L and a pH value of ~8.5 which is identical to that found in the pore solution of α-HH.

Calcium phosphate was precipitated in 50-mL centrifuge tubes through addition of definite volumes of Ca^{2+} solutions to 25 mL of the polyphosphate solutions. The tubes were shaken in a tumbler for 2 h to reach a state of equilibrium. Then the samples were centrifuged for 10 min at 8500 rpm, the supernatant was decanted and the solids were washed with 5 mL DI water and centrifuged twice again. Finally, the residues were dried for 2 days at 60 °C in a drying oven and then weighed.

2.2.9. Precipitation of gypsum from supersaturated solution

To investigate the influence of the polyphosphates on the start of gypsum crystallization, a solution supersaturated with respect to $CaSO_4 \cdot 2H_2O$ was simulated by combining equimolar amounts of $Ca(NO_3)_2$ and Na_2SO_4 respectively. 47.2 g $Ca(NO_3)_2 \cdot 4H_2O$ was dissolved in DI water and filled up to 100 mL in a volumetric flask to obtain a 2 M solution. Similarly, 14.2 g of Na_2SO_4 was dissolved separately to obtain a 1 M solution. 86.5 mL of DI water was stirred in a

flask and simultaneously 4.5 mL of the 2 M $Ca(NO_3)_2$ solution and 9 mL of the 1 M Na_2SO_4 solution were combined. To determine the onset of gypsum crystallization which is indicated by a drop in conductivity, time-dependent conductivity was measured (*Qcond 2200*) under constant stirring of the solution.

3. Results and discussion

3.1. Characterization of the sodium polyphosphate samples

In this study, three different polyphosphate samples designated as PP4, PP6 and PP12 were used and characterized. First, their average chain length (average amount of phosphate groups present in the chain) was determined by liquid ^{31}P NMR spectroscopy. Fig. 2 shows as an example the spectrum of the sample PP4.

For all samples, the spectra show two main groups of signals at approximately −6 ppm and −20 ppm respectively. They can be assigned to the different chemical environments of terminal (Q^1) and bridging (Q^2) phosphorus atoms [22]. The very low intensity of the Q^0 signal at +2 ppm representing orthophosphate signifies the high purity of the samples. Cyclic polyphosphates (Q^2 at −23 ppm) were not detected in significant amounts, thus indicating that the samples were indeed linear polyphosphates. It should be noted that crosslinked (Q^3) polyphosphates cannot be detected via liquid NMR spectroscopy because they undergo immediate hydrolysis when dissolved in D_2O. This behavior is in contrast to linear and cyclic polyphosphates which maintain their structure when dissolved. The presence of crosslinked polyphosphates is however very unlikely, considering the manufacturing process of the samples.

From integration of the signals, the ratio of terminal to bridging phosphorus atoms was determined. Using this method, for each polyphosphate the average chain length was calculated and the samples were designated accordingly. The result is shown in Table 1. According to this, the polyphosphates contain the anions $P_4O_{13}^{6-}$ (in PP4), $P_6O_{19}^{8-}$ (in PP6) and $P_{12}O_{37}^{14-}$ (in PP12) respectively. Note that polyphosphates generally show a chain length distribution, similar to organic polymers, and are not monodispers.

Additionally, via elemental analysis the weight ratio of Na_2O/P_2O_5 was determined and from this the molar ratio between sodium and phosphorus was calculated. Based upon these values, the approximate compositions and molecular weights of the polyphosphate samples were derived, assuming that remaining charges are compensated by protons.

It is generally established that the weight ratio of Na_2O/P_2O_5 or of Na_2HPO_4/NaH_2PO_4 present in the manufacturing process of the polyphosphate is the critical parameter which determines the chain length of a polyphosphate obtained from this process. The reason is that only≡P–O–H groups can form a chain through condensation reaction, while≡P–ONa groups cannot undergo such condensation reaction. Thus, the higher the sodium content in the starting material, the more chain termination takes place and the shorter the chain. This effect is confirmed by the data shown in Table 1. Therefore, the polyphosphate sample exhibiting the highest molar ratio of sodium to phosphorus (PP4) possesses the shortest chain length which is made up of four phosphate units only. Oppositely, PP12 exhibits the lowest molar ratio of Na_2O/P_2O_5 and thus exhibits the longest chain of all samples tested.

Table 1
Composition and properties of the polyphosphate samples used in the study.

Poly-phosphate sample	Average chain length (no. of phosphate groups)	Weight ratio Na_2O/P_2O_5	Molar ratio Na/P	Approximate composition of polyphosphate	Average molecular weight (g/mol)
PP4	4	0.640	1.08	$\sim Na_{4.3}H_{1.7}P_4O_{13}$	~430
PP6	6	0.545	0.91	$\sim Na_{5.5}H_{2.5}O_{19}$	~620
PP12	12	0.481	0.82	$\sim Na_{9.8}H_{4.2}P_{12}O_{37}$	~1200

3.2. Retarding efficiency of the polyphosphates

Generally, hydration of α-$CaSO_4 \cdot 0.5H_2O$ (α-HH) to calcium sulfate dihydrate (DH) involves a three step process: First, α-HH dissolves in water, thus generating a pore solution in which the calcium and sulfate concentrations increase steadily over time until a state of supersaturation with respect to DH is attained [23]. This step is followed by precipitation of DH nuclei from the supersaturated solution [24]. Note that at room temperature, the solubility of DH (~2.05 g/L) is considerably lower than that of α-HH (~8 g/L).The final step is the crystal growth of DH nuclei [25–27]. Mostly, needle shaped DH crystals are formed which entangle and form a dense material exhibiting high strength [28].

Hydration of hemihydrate releases heat due to the exothermic character of the reaction. Thus, hydration kinetics can easily be tracked through isothermal heat flow calorimetry. Fig. 3 displays results from measurements obtained from blank α-HH pastes and pastes containing 0.025% bwob of the individual polyphosphates.

For the reference binder system (no polyphosphate present), a strong heat flow occurs within minutes after mixing. It indicates early beginning of hydration and reaches a maximum after ~40 min. After ~4 h, heat flow decreases to zero, thus indicating the end of the main hydration reaction. In comparison, the hemihydrate pastes which were mixed with polyphosphates do not exhibit any heat development within the first hours. Only after ~3 h, sample PP12 exhibits beginning of a heat flow which reaches a maximum after ~10 h. Samples PP6 and PP4 reach maximum heat flow at 12.5 h and 14 h, respectively. The results indicate that all polyphosphate

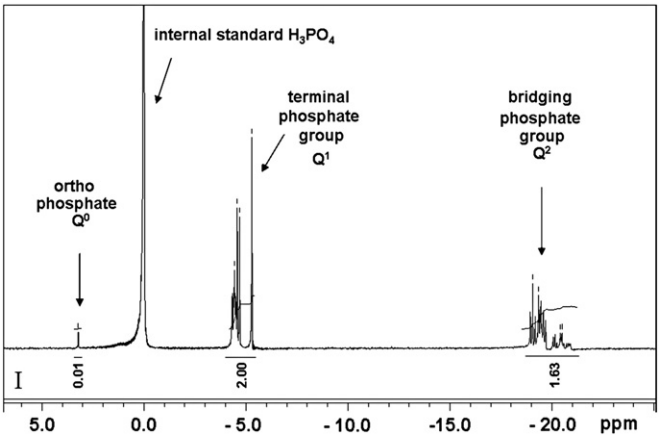

Fig. 2. ^{31}P NMR spectrum of polyphosphate sample PP4, recorded in D_2O.

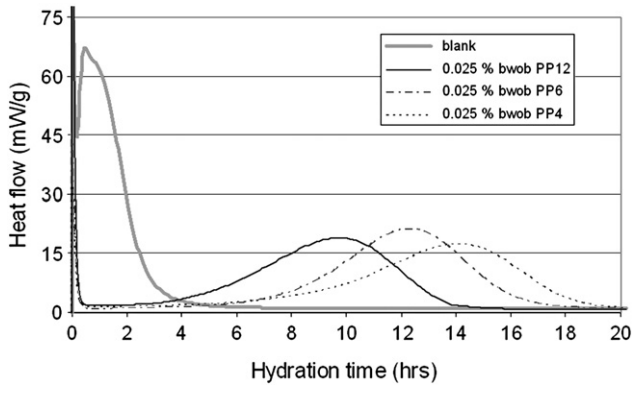

Fig. 3. Time-dependent heat flow of hemihydrate/water suspensions, measured in the absence and presence of different polyphosphate samples.

samples tested present strong retarders, and that the retarding efficiency decreases with increasing chain length.

3.3. Time-dependent degree of hydration

In order to further quantify the retarding efficacy of the polyphosphates, time-dependent degree of hydration of α-$CaSO_4 \cdot 0.5H_2O$ in the presence of each polyphosphate sample was determined at application conditions. The degree of hydration (DoH) was defined as percentage of α-HH converted into DH.

As is shown in Fig. 4, in the absence of polyphosphates DH formation commences within minutes after mixing the α-HH with water. After 30 min, already more than 50% of the binder has been converted into DH. A DoH of over 90% was accomplished within 2 h.

In the presence of any polyphosphate sample, DH formation is delayed significantly. For PP12, the onset of hydration is observed after ~40 min only, for PP6 it occurs after ~60 min and in presence of PP4 even after ~80 min. However, once hydration is initiated, it proceeds at a rate comparable with that for the reference paste free of polyphosphate. Obviously, polyphosphates delay the initial set of α-HH. In this respect, their behavior is similar to that of iminodisuccinate [29,30] and Retardan® (a commercial pyrrolidone formaldehyde polycondensate) [18,31]. The main difference to these additives is the higher efficiency of the polyphosphates at the low dosages employed here.

The results clarify that polyphosphates generally inhibit binder dissolution, early nucleation and/or crystal growth of DH. Their retarding effectiveness generally depends on the chain length. Short chain polyphosphates are more powerful retarders than polyphosphates possessing longer chains.

3.4. Impact on paste workability

Hydration of α-$CaSO_4 \cdot 0.5H_2O$ is generally accompanied by a rapid and substantial increase in paste viscosity. Initial setting of the paste occurs within minutes after the addition of water. By employing retarders, initial and/or final setting can be delayed.

In order to quantify the impact of the retarders on paste fluidity, time dependent paste flow values were taken in the presence and absence of the polyphosphates. This experiment describes the effectiveness of the retarders from the viewpoint of applicators.

As can be seen from Fig. 5, the initial paste flow of the hemihydrate/water suspension (no polyphosphate present) is 17.5 cm and then decreases rapidly within the first 10 min. In contrast to this, the pastes containing any of the polyphosphate samples (dosage: 0.025% bwob) maintain high fluidity over a considerably longer period of time (45–75 min, depending on the sample). Polyphosphate sample PP4 exhibits the strongest retarding effect. Therefore, paste

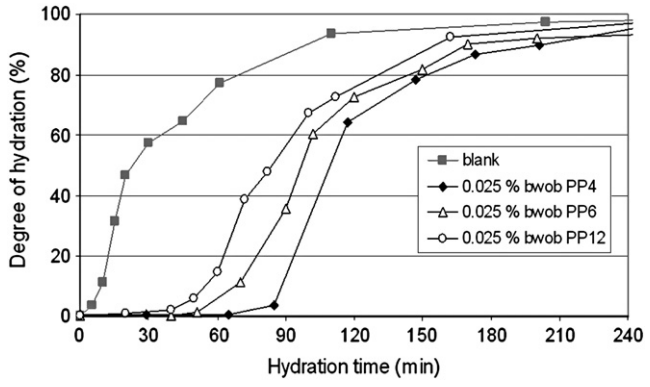

Fig. 4. Time dependent evolution of the degree of hydration of α-$CaSO_4 \cdot 0.5H_2O$ in the absence and presence of different polyphosphate samples.

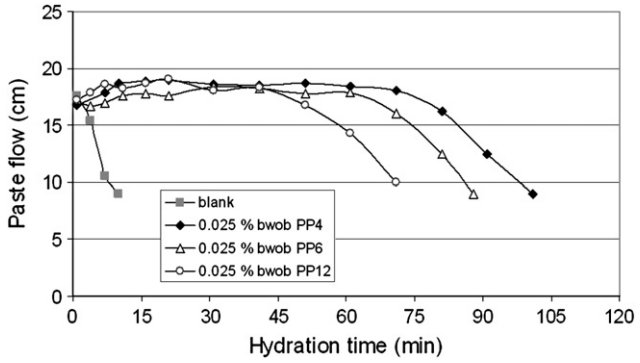

Fig. 5. Paste flow of α-$CaSO_4 \cdot 0.5H_2O$ pastes (w/b ratio 0.33) as a function of time in the absence and presence of different polyphosphate samples.

flow starts to decrease after ~75 min only. PP6 and PP12 retain paste fluidity over periods of 60 min and 45 min, respectively.

The results clearly demonstrate the high retarding capability of the polyphosphate samples. Note the very low dosages of the polyphosphates (0.025% bwob) at which the tests were performed. It also became evident that polyphosphates with shorter chains are more effective retarders than those possessing longer chains. Besides, all polyphosphates exhibit a slight dispersing effect (see Fig. 5).

3.5. Effect on mechanical properties

To evaluate the impact of the polyphosphates on the mechanical properties of the hardened gypsum samples, time-dependent development of the compressive and bending tensile strengths was measured. The results are shown in Table 2.

The results indicate that only after 3 days, all three polyphosphate samples slightly affect both tensile and compressive strength development. The decreases lie between 5 and 10%. After 7 days and longer periods of time, however, no significant differences were found, considering the usual margin of error for such tests.

3.6. Interaction of polyphosphates with calcium ions

To gain more insight into the fundamental processes underlying the retardation effect, interaction of the polyphosphates with Ca^{2+} ions was studied next. For this purpose, 100 mL of 0.1 wt.% polyphosphate solutions was titrated with an aqueous $CaCl_2$ solution which contained 10 g/L of Ca^{2+} ions. To simulate the environment existing in the pore solution of α-HH paste, the pH of the $CaCl_2$ solution was adjusted to 8.5 using aqueous NaOH.

Fig. 6 shows the change in pH occurring when Ca^{2+} ions are introduced into the solutions. For DI water (no polyphosphate present), the pH increases from ~6 to 6.7 as $CaCl_2$ solution is fed in. The change in pH value is the result of the slightly alkaline pH (8.5) of the $CaCl_2$ solution. For the 0.1 wt.% polyphosphate solutions, the initial pH values were 9.2 (PP4), 7.9 (PP6) and 7.4 (PP12), respectively. Those differences in the initial pH values are due to the different acidities of bridging (Q^2) and terminal (Q^1) ≡P–OH groups. Generally, terminal ≡P–OH groups exhibit a considerably higher pK_s value than secondary ≡P–OH groups [32]. The ratio of Q^2/Q^1 phosphorus atoms increases with increasing chain length of the polyphosphate. Thus, acidity of a polyphosphate generally increases with increasing chain length.

Addition of $CaCl_2$ solution strongly decreases the pH of all polyphosphate solutions. This is due to the fact that at first, polyphosphates are not completely dissociated in solution. A significant amount of protons and sodium ions is still coordinated to the phosphate groups [32]. Introducing calcium ions displaces these protons which are then released into the solution. The result of this

Table 2
Development of compressive and tensile strength of α-hemihydrate pastes (w/b ratio = 0.33) in absence and presence of individual polyphosphate samples.

Paste (polyphosphate dosage: 0.025% bwob)	Compressive strength [N/mm²]			Tensile strength [N/mm²]		
	3 days	7 days	28 days	3 days	7 days	28 days
blank	21.3 ± 1.8	33.0 ± 1.2	30.1 ± 2.0	5.9 ± 0.5	11.3 ± 1.0	12.0 ± 0.6
PP4	18.9 ± 1.5	32.5 ± 1.1	30.3 ± 1.7	5.2 ± 0.6	10.4 ± 1.2	11.3 ± 1.3
PP6	20.4 ± 1.0	35.4 ± 1.8	32. 8 ± 2.0	5.9 ± 0.9	11.3 ± 0.8	11.6 ± 0.9
PP12	19.3 ± 1.1	32.6 ± 2.0	29.6 ± 1.8	5.1 ± 0.4	11.0 ± 2.0	11.5 ± 1.1

interaction with Ca^{2+} is a decrease of the pH value of the solution. The experiment allows concluding that Ca^{2+} ions coordinate to oxygen atoms present in the polyphosphates.

Furthermore, during titration with aqueous $CaCl_2$ solution, the polyphosphate solutions first turn into a milky sol containing amorphous calcium polyphosphate particles which exhibit an average diameter of 25–100 nm, as measured by dynamic light scattering. Once a saturation dosage relative to calcium ions is reached and the sequestration ability of the polyphosphate is exhausted, initially formed turbid calcium polyphosphate sol undergoes gelation into a viscous fluid, as is typical for sol–gel transformation [33]. Apparently, the calcium ions function as a crosslinker between non-bridging oxygen atoms present in different polyphosphate molecules [34]. Through these linkages, a gel made up of a 3D network is formed.

Next, the onset of turbidity during $CaCl_2$ titration was measured as a function of the concentration of calcium ions added. The results are exhibited in Fig. 7.

For the 0.1 wt.% (0.33 mmol) PP4 solution, the first precipitate occurred after addition of 1.25 mL of $CaCl_2$ solution. This volume corresponds to a dosage of 0.313 mmol Ca^{2+}. Further addition of Ca^{2+} ions led to a sharply increased turbidity. For the PP6 and PP12 solutions, the onset of turbidity was observed at higher $CaCl_2$ additions (for 0.16 mmol PP6: at 1.6 mL $CaCl_2$ solution which corresponds to 0.4 mmol Ca^{2+}; for 0.083 mmol PP12: at 3.2 mL $CaCl_2$ solution, corresponding to 0.8 mmol Ca^{2+}). Apart from these different onset concentrations, the general behavior of all polyphosphate samples was comparable.

The results confirm that short-chain polyphosphates such as PP4 form calcium precipitates at lower Ca^{2+} concentrations than long-chain polyphosphates.

To quantify the amount of precipitate, the solids formed after addition of different amounts of $CaCl_2$ solution were equilibrated for 2 h and then collected via centrifugation, washed twice with DI water, dried and weighed. All precipitates were completely X-ray amorphous and exhibited no reflections in powder diffractograms.

Quantitation showed that the amounts of precipitate formed differ significantly for the three polyphosphates (Fig. 8). From the PP4 solution, a total of 103 mg of calcium polyphosphate precipitate was collected. This corresponds to nearly 100% precipitation of the phosphate. The other polyphosphates were only partially deposited from the solution. From PP6, 50% and from PP12 only 10% of present polyphosphate were precipitated. This effect is due to the different chain length distributions of the polyphosphates. The short chain fraction of the polyphosphates precipitates while longer chained polyphosphate molecules stay in solution. Thus, the longer the average chain length, the smaller is the amount of precipitated short chained polyphosphates. Interestingly, for all polyphosphates completeness of precipitation was achieved at the same added volume of ~7.5 mL $CaCl_2$ solution (this corresponds to 1.88 mmol Ca^{2+} or a concentration of 0.7 g/L Ca^{2+}, respectively).

In summary, the interaction between calcium and polyphosphate starts with coordination of Ca^{2+} ions to oxygen atoms present in the polyphosphates and proceeds with the formation of insoluble, neutral and nano-sized calcium phosphate sol particles which can undergo condensation into a gel. Short-chain polyphosphates form calcium precipitates at lower Ca^{2+} concentrations and react more completely than long-chain phosphates. For this reason, short-chain polyphosphates are more effective retarders than those possessing long chains. This behavior explains the results obtained for the degree of hydration (Fig. 4) and in the mini slump tests (Fig. 5).

3.7. Working mechanism of polyphosphate retarders

To investigate the retarding mechanism of the polyphosphates in greater detail, their interaction with Ca^{2+} ions was studied relative to individual steps occurring during hydration of α-HH.

3.7.1. Impact on binder dissolution

The first step in the hydration of α-HH involves the dissolution of the binder. This process can be tracked quantitatively by conductometry. Here, the tests were carried out at a water-to-binder ratio of 20:1. Additionally, through simultaneous determination of the degree of hydration, the progress of hydration was monitored.

Plain α-HH (no polyphosphate present) exhibited the typical hydration behavior known for this type of binder (see Fig. 9). In the first 10 min, conductivity of the paste increases strongly as a result of binder dissolution which releases calcium and sulfate ions into

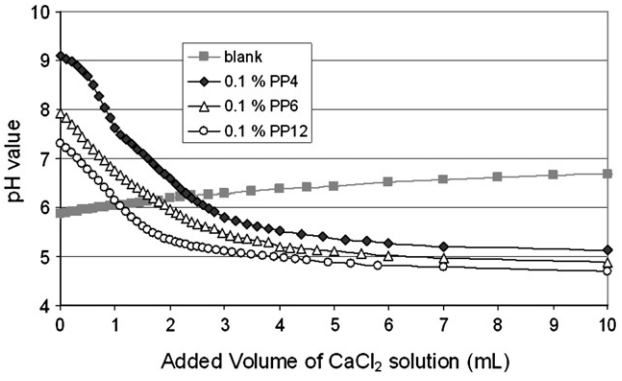

Fig. 6. Evolution of pH values of 0.1 wt.% polyphosphate solutions during titration with aqueous 3.675 wt.% $CaCl_2 \cdot 2H_2O$ solution.

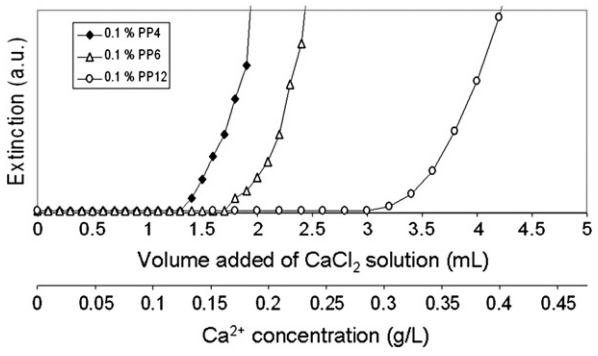

Fig. 7. Onset point for occurrence of turbidity of 0.1 wt.% polyphosphate solutions combined with increased volumes of $CaCl_2$ solution.

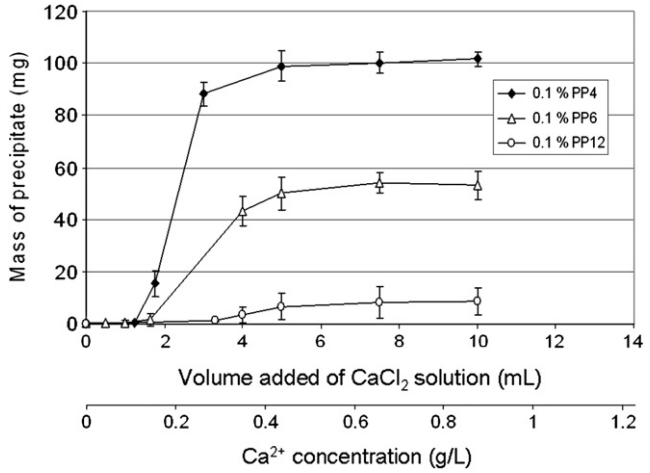

Fig. 8. Amount of precipitate collected from individual 0.1 wt.% polyphosphate solutions after titration with increasing volumes of $CaCl_2$ solution.

solution. After reaching a value of ~5 mS/cm, conductivity remained constant for about 25 min. The Ca^{2+} concentration present at this time corresponds to ~2.4 g/L. During this period, DH nuclei start to evolve and grow into larger crystals which then precipitate. Conductivity remains nearly constant in this period because DH is precipitated from the supersaturated solution at the same rate at which the binder dissolves. Only when α-HH is close to exhaustion, conductivity decreases and within 30 min, a constant conductivity value of about 2 mS/cm is reached which corresponds to saturation relative to DH. This indicates that hydration of α-HH has reached completeness now.

In the presence of polyphosphates, however, a completely different course of hydration is observed (Fig. 10). Similar to plain α-HH, conductivity of all polyphosphate suspensions rises within in the first minutes, yet at a much lower rate. After 30 min only, a conductivity value of ~4 mS/cm is attained which compares with ~2 min for the pure α-HH system to reach this conductivity value. Much different to the α-HH sample, conductivity of the suspensions holding the polyphosphates steadily increases over the entire test period of 120 min. Slight differences between the polyphosphate samples can be seen in that for PP4, conductivity is generally lower than for PP6 or PP12. For all polyphosphate suspensions, the degree of hydration remained below 10%, thus signifying that precipitation and crystallization of DH have not occurred much during the 120 min period.

This result allows concluding that linear polyphosphates inhibit the dissolution of α-HH. The state of supersaturation which is required to initiate crystallization of DH is significantly delayed. Obviously, calcium ions dissolved from the binder react with the polyphosphates to form an amorphous precipitate (as was shown

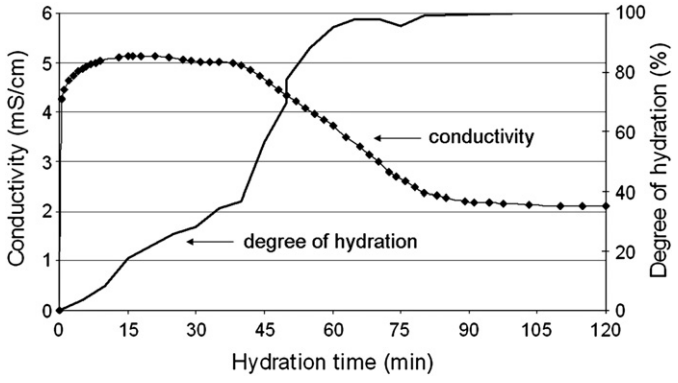

Fig. 9. Time-dependent evolution of conductivity and respective degree of hydration for α-$CaSO_4 \cdot 0.5H_2O$ suspended in water (w/b = 20).

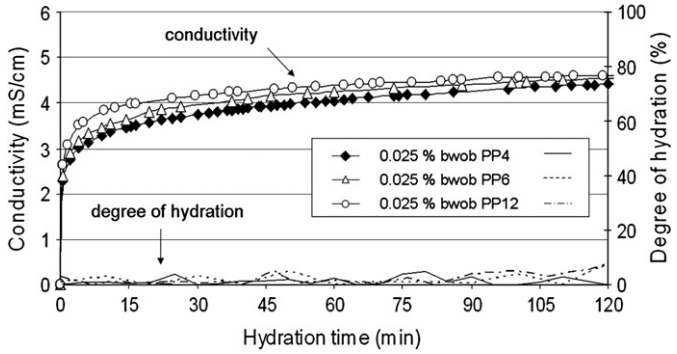

Fig. 10. Time-dependent evolution of conductivity and degree of hydration for aqueous α-$CaSO_4 \cdot 0.5H_2O$ suspensions (w/b = 20) holding the polyphosphate samples.

before) which covers the binder surface and inhibits its further dissolution. This model was confirmed by the observation that the concentration of calcium ions found in the pore solution (> 2 g/L Ca^{2+}) soon exceeded that one needed for maximum precipitation of the polyphosphates (0.7 g/L Ca^{2+}; see Fig. 8). To our knowledge, in calcium sulfate systems inhibition of binder dissolution has so far only been reported for cellulose ethers. They were shown to increase the viscosity of the pore solution such that dissolution of the ions from the surface of the binder is impacted [35].

Next, time dependent depletion of polyphosphate from the pore solution was studied. The result is presented in Fig. 11. Within 30 s, all three polyphosphates are nearly quantitatively precipitated. Again, slight differences between the polyphosphate samples are apparent. PP4 is depleted faster and to a larger extent than PP6 and PP12, respectively.

As was shown before in Fig. 8, PP6 and PP12 are not precipitated quantitatively in the presence of Ca^{2+} ions. But in this test, their depletion from solution approaches ~90%. This signifies that polyphosphates which are not precipitated adsorb onto the surface of the binder or of calcium phosphate precipitates formed, respectively. Other authors have established that for polyphosphates, precipitation and sorption are more preferred processes than formation of their Ca^{2+} complexes [36].

3.7.2. Supersaturation and crystal growth

Continuous dissolution of calcium and sulfate ions results in a solution which is supersaturated relative to DH. From there, gypsum crystals precipitate. To evaluate the effect of the polyphosphates on this hydration step, a supersaturated $CaSO_4 \cdot 2H_2O$ solution was prepared by combining 0.09 M $Ca(NO_3)_2$ and 0.09 M Na_2SO_4 solutions. The stability of the solution and the time elapsed until gypsum

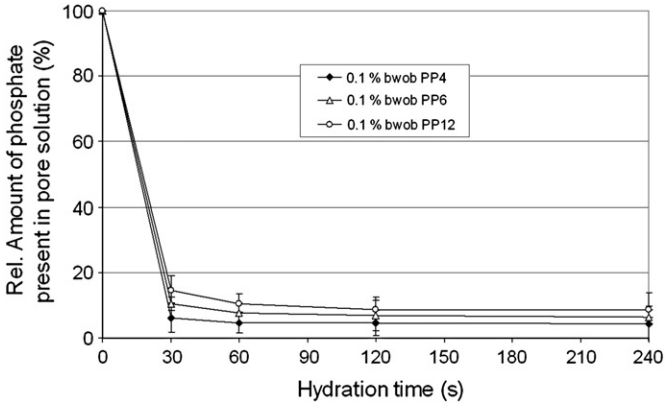

Fig. 11. Relative amount of polyphosphate present in the pore solution of α-HH paste as a function of hydration time (w/b ratio = 0.33).

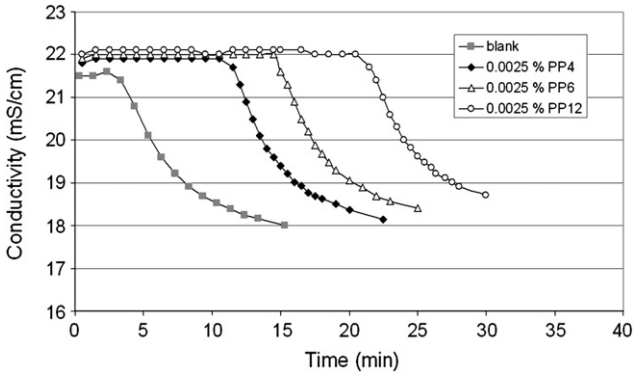

Fig. 12. Time dependent conductivity of combined equimolar $Ca(NO_3)_2/Na_2SO_4$ solutions in the absence and presence of polyphosphates.

formation occurred were tracked by conductivity. The results are displayed in Fig. 12.

The equimolar mixture of $Ca(NO_3)_2$ and Na_2SO_4 (no polyphosphate present) initially exhibits a conductivity of approximately 21.5 mS/cm. After ~4 min, a drop in conductivity is observed which is owed to precipitation of gypsum from the solution. In the presence of very small amounts (0.0025 wt.%) of the polyphosphates, however, conductivity of the solutions remained constant for a much longer time period. These samples undergo precipitation and subsequent decrease in conductivity only after ~12 min for PP4, ~15 min for PP6 and ~22 min for PP12, respectively.

Accordingly, polyphosphates inhibit precipitation of gypsum already at understoichiometric concentrations relative to their neutral calcium complexes. Theoretically, assuming complete charge compensation, the polyphosphates can bind 3 (PP4), 4 (PP6) or 7 (PP12) Ca^{2+} ions per molecule, respectively. However, here the Ca^{2+} to polyphosphate molar ratios are considerably higher, namely 1550 (PP4), 2250 (PP6) and 4500 (PP12). This signifies that extremely low dosages of polyphosphate are capable to bind enormous quantities of calcium. This effect is known as "threshold effect" and presents the basic mechanism underlying the application of polyphosphates as scale inhibitors [37]. The "threshold effect" relies on adsorption of polyphosphates onto the surface of emerging crystal nuclei and subsequent blocking of their further growth. Therefore, already at ultra-low concentrations of such threshold agents, precipitation is inhibited.

Note the opposite order of efficacy for the polyphosphate samples in this test (Fig. 12), compared to the degree of hydration (Fig. 4), paste flow (Fig. 5) and calcium precipitation experiments (Figs. 7 and 8). In the test on calcium binding capability, long-chain polyphosphate samples exhibit higher threshold ability than those possessing shorter chains. This behavior explains why the detergent industry preferably uses very long chain polyphosphates. These were excluded from the present study because preliminary screening tests revealed inferior retarding efficacy than for the short-chain polyphosphates tested here.

4. Conclusions

The study confirms that linear sodium polyphosphates strongly influence various steps involved in the hydration of α-HH. At remarkably low dosages (0.025% bwob), the time period in which the binder paste remains fluid and possesses sufficient workability is significantly extended. Accordingly, polyphosphates act as strong set retarders. After 3 days, strength development of α-HH specimens is only slightly reduced by the phosphates while after longer curing periods, no more difference is observed.

The retarding mechanism of polyphosphates relies on multiple interactions: First, dissolved polyphosphate reacts with solved Ca^{2+} ions to produce a precipitate of calcium polyphosphate which covers the surface of the binder and hinders its further dissolution. Second, the state of supersaturation relative to gypsum is stabilized by the presence of polyphosphates ("threshold effect") and the onset of gypsum crystallization is delayed. An almost complete removal of the polyphosphates from the pore solution as a result of Ca^{2+} presence proves that both precipitation and surface adsorption of the polyphosphates occur simultaneously. To summarize, the rate of dissolution of α-HH is decelerated, Ca^{2+} is kept in solution through complexation, and the growth of initial DH crystals is impeded by polyphosphate adsorption.

The effects described vary with the average chain length of the polyphosphate sample. In the presence of calcium ions, short-chain polyphosphates precipitate earlier and are more complete. Owing to this effect, they exhibit a stronger influence on the rate of dissolution of the binder. Long-chain polyphosphates, however, possess higher threshold abilities and thus better stabilize the supersaturated $CaSO_4 \cdot 2H_2O$ solution. The overall higher retarding effectiveness of short-chain polyphosphates as demonstrated in the mini slum tests confirms that inhibition of binder dissolution prevails over stabilization of the state of supersaturation. Consequently, the first effect presents the key process in the retarding mechanism of linear polyphosphates.

Acknowledgments

The authors would like to thank Erwin Schmidt and Chemische Fabrik Budenheim for providing the polyphosphate samples. Prof. H.-U. Hummel and Knauf Gips KG are thanked for the supply of α-calcium sulfate hemihydrate.

References

[1] T. Staffel, Phosphoric Acid and Phosphates, 5th ed., Ullmann's Encyclopedia of Industrial Chemistry, Vol. A 19, 2002.
[2] E.J. Griffith, Chemical and physical properties of condensed phosphates, Pure Appl. Chem. 44 (2) (1975) 173–200.
[3] M. Nakagaki, H. Inoue, T. Fujie, S. Ohashi, The polymerization reaction of sodium phosphate, Bull. Chem. Soc. Jpn. 36 (5) (1963) 595–599.
[4] K.G. Cooper, L.G. Hanlon, G.M. Smart, R.E. Talbot, 25 years experience in the development and application of scale inhibitors, Desalination 31 (1–3) (1979) 243–255.
[5] I.S. Kulaev, V.M. Vagabov, T.V. Kulakovskaya, The Biochemistry of Inorganic Polyphosphates, John Wiley & Sons, Chichester, UK, 2004.
[6] A. Papo, L. Piani, R. Ricceri, Sodium phosphates as dispersing agents for calcium carbonate industrial slurries: rheological characterization, Silic. Indus. 68 (9–10) (2003) 119.
[7] L. Huynh, D.A. Beattie, D. Fornasiero, J. Ralston, Effect of polyphosphate and naphthalene sulfonate formaldehyde condensate on the rheological properties of dewatered tailings and cemented paste backfill, Miner. Eng. 19 (1) (2006) 28–36.
[8] J.W. Lyons, Distribution of polyphosphate deflocculants in aqueous suspensions of inorganic solids, in: E.J. Griffith (Ed.), Environmental Phosphorus Handbook, John Wiley & Sons, New York, 1973, pp. 56–75.
[9] J.W. Lyons, Sodium tri(poly)phosphate in the kaolinite–water system, J. Colloid Sci. 19 (5) (1964) 399–412.
[10] G. Lagaly, S. Ziesmer, Colloid chemistry of clay minerals: the coagulation of montmorillonite dispersions, Adv. Colloid Interface Sci. 100–102 (2003) 105–128.
[11] H.C.H. Darley, G.R. Gray, Composition and Properties of Drilling and Completion Fluids, Sixth Edition, Gulf Professional Publishing, 2011.
[12] M. Singh, M. Garg, Retarding action of various chemicals on setting and hardening characteristics of gypsum plaster at different pH, Cem. Concr. Res. 27 (6) (1997) 947–950.
[13] E. Badens, S. Veesler, R. Boistelle, Crystallization of gypsum from hemihydrate in presence of additives, J. Cryst. Growth 198 (1999) 704–709.
[14] J.-R. Hill, J. Plank, Retardation of setting of plaster of Paris by organic acids: understanding the mechanism through molecular modeling, J. Comput. Chem. 25 (12) (2004) 1438–1448.
[15] A. Ersen, A. Smith, T. Chotard, Effect of malic and citric acid on the crystallisation of gypsum investigated by coupled acoustic emission and electrical conductivity techniques, J. Mater. Sci. 41 (21) (2006) 7210–7217.
[16] C. Vellmer, B. Middendorf, N.B. Singh, Hydration of alpha-hemihydrate in the presence of carboxylic acids, J. Therm. Anal. Calorim. 86 (3) (2006) 721–726.
[17] B. Middendorf, C. Vellmer, M. Schmidt, Take a closer look: calcium sulfate based building materials in interaction with chemical additives, International Symposium on Nanotechnology in Construction, Paisley, Scotland, 2003.
[18] T. Mallon, Retarding action of gypsum plaster retarders of various chemical composition in relation to the pH value of the plaster, ZKG 41 (6) (1988) 309–311.

[19] H. Reul, Untersuchungen an Stuck- und Maschinenputzgips mit Verzögerern auf Oxy-Carbonsäure- und Eiweißbasis, ZKG 7 (1977) 331–333.
[20] S.R. Crouch, H.V. Malmstad, A mechanistic investigation of molybdenum blue method for determination of phosphate, Anal. Chem. 39 (10) (1967) 1084–1089.
[21] A. Sjosten, S. Blomqvist, Influence of phosphate concentration and reaction temperature when using the molybdenum blue method for determination of phosphate in water, Water Res. 31 (7) (1997) 1818–1823.
[22] M.M. Crutchfield, C.F. Callis, R.R. Irani, G.C. Roth, Phosphorus nuclear magnetic resonance studies of ortho and condensed phosphates, Inorg. Chem. 1 (4) (1962) 813–817.
[23] U. Ludwig, N.B. Singh, Hydration of hemihydrate of gypsum and its supersaturation, Cem. Concr. Res. 8 (3) (1978) 291–299.
[24] P.G. Klepetsanis, P.G. Koutsoukos, Spontaneous precipitation of calcium-sulfate at conditions of sustained supersaturation, J. Colloid Interface Sci. 143 (2) (1991) 299–308.
[25] L. Amathieu, R. Boistelle, Crystallization kinetics of gypsum from dense suspension of hemihydrate in water, J. Cryst. Growth 88 (2) (1988) 183–192.
[26] F.W. Birss, T. Thorvaldson, The hydration of plaster of Paris, Can. J. Chem. 33 (5) (1955) 870–880.
[27] M.J. Ridge, J. Beretka, Calcium sulfate hemihydrate and its hydration, Rev. Pure Appl. Chem. 19 (3) (1969) 17–22.
[28] N.B. Singh, B. Middendorf, Calcium sulfate hemihydrate hydration leading to gypsum crystallization, Prog. Cryst. Growth Charact. Mater. 53 (1) (2007) 57–77.
[29] H. Reul, Zur Wirkung von Iminodisuccinat als Verzögerer von Maschinenputzgipsen, ZKG Int. 9 (1999) 522–526.
[30] T. Staffel, T. Klein, G. Brix, F. Wahl. Verfahren zur Abbindeverzögerung von Gips und Gipszubereitungen, 2001, Patent DE 10017133A1; BK Giulini Chemie GmbH & Co. oHG.
[31] J. Schneider, D. Freyer, W. Voigt, The effect of retarders on the setting process in industrially relevant hemihydrate gypsum plasters, ZKG Int. 60 (12) (2007) 68–76.
[32] J.R. Van Wazer, K.A. Holst, Structure and properties of the condensed phosphates. I. Some general considerations about phosphoric acids I, J. Am. Chem. Soc. 72 (2) (1950) 639–644.
[33] N.C. Masson, E.F. Desouza, F. Galembeck, Calcium and iron(III) poly-phosphate gel formation and aging, Colloids Surf. A 121 (2–3) (1997) 247–255.
[34] I. Ahmed, M. Lewis, I. Olsen, J.C. Knowles, Phosphate glasses for tissue engineering: Part 2. Processing and characterisation of a ternary-based P_2O_5–CaO–Na_2O glass fibre system, Biomaterials 25 (3) (2004) 501–507.
[35] F. Brandt, D. Bosbach, Bassanite ($CaSO_4 \cdot 0.5H_2O$) dissolution and gypsum ($CaSO_4 \cdot 2H_2O$) precipitation in the presence of cellulose ethers, J. Cryst. Growth 233 (4) (2001) 837–845.
[36] J.R. Van Wazer, Phosphorus and Its Compounds, Vol. 1: Chemistry, Interscience Publishers, Inc., New York, 1985.
[37] M.N. Elliot, Scale control by threshold treatment, Desalination 8 (2) (1970) 221–236.